Transonic Panel Method for the Full Potential Equation Applied to Multicomponent Airfoils

B. Oskam*
National Aerospace Laboratory (NLR), Amsterdam, the Netherlands

The panel method approach is extended to obtain numerical solutions of the full potential equation for transonic flow. This extension is accomplished by adding a field distribution of source singularities to the conventional distribution of singularities over the boundaries of the field. The unknown source distribution in the field is determined by solving the full potential equation. Shock waves are captured automatically by splitting the transformed flux components and applying upwind differencing to the monotonic, supersonic parts. The transonic panel method limits the space discretization to those parts of the flow domain in which the nonlinear compressibility effects are non-negligible. The method is tested by computing the potential flow over single- and multicomponent airfoils.

I. Introduction

THE first three-dimensional panel method solving incompressible potential flow problems was introduced two decades ago by Hess and Smith.[1] The most significant capability offered by panel methods is the treatment of complicated, multicomponent geometries (e.g., complete aircraft configurations) without any need for grid generation in the multiply connected domain surrounding the configuration.

Finite difference methods have been able to treat the full potential equation in the nonlinear regime, but require the construction of a body-fitted grid in the complete flow domain.

The subject of this paper is the extension of subsonic panel methods to transonic flows with shocks. In this approach, space discretization is limited to those parts of the flow in which the nonlinear compressibility effects are non-negligible. The idea is to represent the nonlinear compressibility effect by means of a source distribution in space. Previous investigators[2-8] have also worked with distributed singularities in the external flowfield. These methods are usually referred to by such names as field panel methods, integral representation methods, or transonic panel methods. The development of these techniques is far from complete. The present method handles both multicomponent airfoils, as well as transonic flows with shock waves, and is part of a more general research effort directed toward the development of a second-generation panel method[9,10] for nonlinear compressible flow computation employing multigrid-type solvers.

The purpose of this paper is to present the formulation of the new transonic panel method. It will be shown that the continuous boundary value problem can be reformulated in terms of unknown, Prandtl-Glauert singularity distributions. The jump conditions of these singularity distributions are discussed in detail, such that the external Neumann boundary condition may be replaced by an interior Dirichlet condition. Moreover it is also shown that the well-established fully conservative finite volume technique,[11] combined with flux splitting,[12-14] can be reformulated in terms of singularity distributions. In the last section, we briefly discuss some of the computational results obtained with a pilot code employing Laplace singularity distributions.

Presented as Paper 83-1855 at the AIAA Applied Aerodynamics Conference, Danvers, Mass., July 13-15, 1983; received Nov. 17, 1983; revision received Oct. 24, 1984.

*Senior Research Engineer, Fluid Dynamics Division. Member AIAA.

II. Boundary Value Problem Formulation

Let the Cartesian coordinates be denoted by x,y,z with unit vectors $\hat{e}_x,\hat{e}_y,\hat{e}_z$, and the full potential by Φ. Then, we may write the full potential equation, in the form of a conservation law for mass flow, as

$$\vec{\nabla}\cdot(\rho\vec{\nabla}\Phi)=0 \tag{1}$$

where the density ρ is defined by

$$\rho=\left[1+\frac{\gamma-1}{2}M_\infty^2(1-\vec{\nabla}\Phi\cdot\vec{\nabla}\Phi)\right]^{1/(\gamma-1)} \tag{2}$$

the two-dimensional del operator by

$$\vec{\nabla}=\hat{e}_x\frac{\partial}{\partial x}+\hat{e}_y\frac{\partial}{\partial y} \tag{3}$$

and where M_∞ denotes the Mach number of the freestream and γ the ratio of the specific heats. Consider the geometry of a multicomponent airfoil with a number of n_c components. The flow tangency condition requires that

$$(\hat{n}\cdot\vec{\nabla}\Phi)_q=0,\quad q\in C_j\quad\text{for}\quad j=1,\ldots,n_c \tag{4}$$

where C_j is the contour of component j and $\hat{n}_q$ the unit outward normal of C_j at q.

The Kutta conditions are expressed by the identity of the upper and lower side limiting values of the tangential velocity components at the trailing edges T_j. The Kutta conditions are expressed by

$$\lim_{q\to T_j}\left[(\hat{t}\cdot\vec{\nabla}\Phi)_{q,\text{upper}}+(\hat{t}\cdot\vec{\nabla}\Phi)_{q,\text{lower}}\right]=0 \tag{5}$$

$$q\in C_j\quad\text{for}\quad j=1,\ldots,n_c$$

where $\hat{t}_q$ denotes the unit tangential vector of C_j at q, $\hat{t}$ being taken positive such that $\hat{n}\times\hat{t}=\hat{e}_z$.

The boundary value problem is completed by the freestream boundary condition at infinity,

$$\Phi(x,y\to\infty)=u_\infty x-\frac{\Gamma}{2\pi}\arctan\left(\sqrt{1-M_\infty^2}\,\frac{y}{x}\right)+\mathcal{O}(x^2+y^2)^{-1/2} \tag{6}$$

where Γ denotes the unknown circulation of the flow and u_∞ the magnitude of the uniform freestream, which is taken along the x axis without loss of generality.

III. Integral Representation

Singularity Distributions

Let the solution Φ of the boundary value problem be expressed as the sum of a uniform flow potential and a perturbation potential φ,

$$\Phi(x,y) = u_\infty x + \varphi(x,y) \tag{7}$$

This perturbation potential is subsequently expressed in terms of a general integral representation that involves not only integrals over the boundaries but also over the domain external to the contours C_j, allowing for the exact representation of the solution Φ of the nonlinear potential flow problem. The kernel of this integral representation is given by the fundamental solution of a linear operator obtained after linearization of the nonlinear full potential equation (1).

Two well-known equations resulting from linearization of Eq. (1) are the Prandtl-Glauert and Laplace equations, both being covered by the linear operator

$$L(\phi) = a^2\phi_{xx} + \phi_{yy} \tag{8}$$

with $a=1$ for the Laplace and $a=\sqrt{1-M_\infty^2}$ for the Prandtl-Glauert operator. The fundamental solution K of Eq. (8) is given by

$$K(p,q) = \ell_n |\vec{r}_{pq}| \tag{9a}$$

$$\vec{r}_{pq} = \frac{1}{a}(x_p - x_q)\hat{e}_x + (y_p - y_q)\hat{e}_y \tag{9b}$$

Using a generalization of Green's theorem, it can be shown that the solution φ of the problem posed by Eqs. (1-7) may be represented by a general potential ϕ,

$$\begin{aligned}\phi(x_p,y_p) = {} & \frac{1}{2\pi}\int\int_D \sigma_q K(p,q)\,\mathrm{d}s_q \\ & + \sum_{j=1}^{n_c}\frac{1}{2\pi}\int_{C_j+W_j} \tau_q K(p,q)\,\mathrm{d}t_q \\ & + \sum_{j=1}^{n_c}\frac{1}{2\pi}\int_{C_j+W_j} \mu_q \hat{n}_q\cdot\tilde{\nabla}_q K(p,q)\,\mathrm{d}t_q\end{aligned} \tag{10}$$

where

C_j = contour of component j
W_j = wake line of component j
D = multiply connected external domain
σ_q = source singularity distribution, $q\in D$
τ_q = source singularity distribution, $q\in C_j$ or W_j
μ_q = doublet singularity distribution, $q\in C_j$ or W_j

The modified del operator is given by

$$\tilde{\nabla}_q = a\hat{e}_x\frac{\partial}{\partial x_q} + \frac{1}{a}\hat{e}_y\frac{\partial}{\partial y_q} \tag{11}$$

The subscript q of the operator above indicates differentiation with respect to (x_q,y_q), assuming (x_p,y_p) is fixed.

Jump Conditions

As mentioned in the Introduction, we will replace the Neumann boundary condition [Eq. (4)] by an equivalent Dirichlet condition. To do this correctly, we will have to evaluate the jump conditions of the doublet and source singularity distributions μ and τ implied by the integrals of Eq. (10). These general jump conditions are different from the well-known Laplacian values.

Consider the perturbation velocity $\vec{v}_\tau$ induced at a point p by a continuous source distribution $\tau_q = \tau(x_q,y_q)$ on a regular curve C,

$$\vec{v}_\tau(x_p,y_p) = \vec{\nabla}_p\phi_\tau = \frac{1}{2\pi}\int_C \tau_q\vec{\nabla}_p K(p,q)\,\mathrm{d}t_q \tag{12}$$

Investigating the limiting behavior of this induced velocity, we shall make use of the unit normal and unit tangent vectors of the curve C,

$$\hat{n} = n_x\hat{e}_x + n_y\hat{e}_y \tag{13a}$$

$$\hat{t} = t_x\hat{e}_x + t_y\hat{e}_y \tag{13b}$$

with

$$\hat{n}\cdot\hat{t} = 0 \text{ or } n_x = t_y,\ n_y = -t_x \tag{13c}$$

It is also convenient to introduce a modified normal vector $\tilde{n}$ such that

$$\tilde{n}\cdot\vec{\nabla} = \hat{n}\cdot\tilde{\nabla} \tag{14a}$$

$$\tilde{n} = a\,n_x\hat{e}_x + (1/a)n_y\hat{e}_y \tag{14b}$$

and a modified tangential vector such that

$$\tilde{n}\cdot\tilde{t} = 0 \text{ and } |\tilde{t}| = |\tilde{n}| \tag{15a}$$

or

$$\tilde{t} = (1/a)t_x\hat{e}_x + a\,t_y\hat{e}_y \tag{15b}$$

From a limiting analysis, it follows that the velocity vector $\vec{v}_\tau$ approaches different limits as the point p approaches q along the normal to C at q from either side. The jump in $\vec{v}_\tau$ at q is given by

$$\vec{v}_\tau^{+}(q) - \vec{v}_\tau^{-}(q) = (1/A_q)\tau_q\hat{n}_q \tag{16a}$$

where A_q denotes the scalar product

$$A_q = \hat{n}_q\cdot\tilde{n}_q \tag{16b}$$

Similarly, it can be shown that the potential ϕ_τ is continuous across C. Thus, the general source singularity τ induces a normal velocity jump that differs only by a factor $1/A_q$ from the Laplacian value.

Before treating the third integral in Eq. (10), it is advantageous to introduce the identity

$$\hat{n}_q\cdot\tilde{\nabla}_q K(p,q) = \hat{t}_q\cdot\vec{\nabla}_q K^*(p,q) \tag{17a}$$

or

$$K^*(p,q) = \arctan\left[a\,\frac{(y_p - y_q)}{(x_p - x_q)}\right] \tag{17b}$$

This identity allows us to integrate the doublet integral of Eq. (10) by parts,

$$\begin{aligned}\phi_d(x_p,y_p) = {} & \frac{1}{2\pi}\int_C \left(\frac{\mathrm{d}\mu}{\mathrm{d}t}\right)_q K^*(p,q)\,\mathrm{d}t_q \\ & + \frac{1}{2\pi}\int_C \mathrm{d}[\mu_q K^*(p,q)]\end{aligned} \tag{18}$$

Letting the point p approach q along the normal to C at q from either side gives

$$\phi_d^+(q) - \phi_d^-(q) = -\mu_q \tag{19}$$

which is identical with the Laplacian case.

The jump in the perturbation velocity vector

$$\vec{v}_d(x_p, y_p) = \vec{\nabla}_p \phi_d(x_p, y_p) \tag{20}$$

induced by a sufficiently smooth doublet distribution μ on a regular curve C is given by

$$\vec{v}_d^+(q) - \vec{v}_d^-(q) = \frac{-1}{A_q}\left(\frac{d\mu}{dt}\right)_q \tilde{t}_q \tag{21}$$

Taking the normal and tangential components of this jump [Eq. (21)] yields

$$\hat{n}_q \cdot [\vec{v}_d^+(q) - \vec{v}_d^-(q)] = -\frac{B_q}{A_q}\left(\frac{d\mu}{dt}\right)_q \tag{22a}$$

$$\hat{t}_q \cdot [\vec{v}_d^+(q) - \vec{v}_d^-(q)] = -\left(\frac{d\mu}{dt}\right)_q \tag{22b}$$

with

$$B_q = \hat{n}_q \cdot \tilde{t}_q \tag{23}$$

Thus, the doublet singularity distribution μ does create a jump across C in the normal derivative of the potential if the scalar product B_q is unequal to zero, which is generally the case. This jump in the normal velocity component [Eq. (22a)] will have to be taken into account if the exact Neumann boundary condition [Eq. (4)] is to be replaced by an equivalent Dirichlet condition at the interior of C.

Equivalent Boundary Conditions

Let us consider the Dirichlet boundary condition at the interior of contour C_j

$$\varphi^-(x_q, y_q) = 0, \quad q \in C_j \text{ for } j = 1, \ldots, n_c \tag{24}$$

This Dirichlet condition is equivalent to the Neumann condition [Eq. (4)] provided we make a specific choice for the source singularity distribution τ_q,

$$\tau_q = B_q\left(\frac{d\mu}{dt}\right)_q - A_q u_\infty \hat{n}_q \cdot \hat{e}_x, \quad q \in C_j \text{ for } j = 1, \ldots, n_c \tag{25}$$

The equivalence of Eq. (4) and Eqs. (24) and (25) follows from the fact that boundary condition (24) leads to the solution

$$\phi(x_p, y_p) = u_\infty x_p \tag{26}$$

at all points p interior to contour C_j for $j = 1, \ldots, n_c$. This solution [Eq. (26)] can be shown to be unique. Substituting the source strength [Eq. (25)] into the jump condition [Eq. (16a)] and adding the jump in normal velocity induced by the doublet singularity [Eq. (22a)] yields a jump in the normal derivative of the full potential that cancels the normal derivative of the unique, interior solution given by Eq. (26), such that we recover the exact Neumann condition given by Eq. (4).

Similarly, we shall also reformulate the Kutta conditions [Eq. (5)] by using the jump conditions. Thus,

$$(\hat{t} \cdot \vec{\nabla}\phi^+)_q = u_\infty \hat{t}_q \cdot \hat{e}_x - \left(\frac{d\mu}{dt}\right)_q \tag{27}$$

and

$$\lim_{q \to T_j}\left[\left(\frac{d\mu}{dt}\right)_{q,\text{upper}} + \left(\frac{d\mu}{dt}\right)_{q,\text{lower}}\right] = \lim_{q \to T_j}[u_\infty(\hat{t}_{q,\text{upper}} + \hat{t}_{q,\text{lower}}) \cdot \hat{e}_x], \quad q \in C_j \text{ for } j = 1, \ldots, n_c \tag{28}$$

Equation (27) gives the contour velocity in terms of μ. The resulting Kutta conditions [Eq. (28)] are explicit conditions for the doublet singularity distribution μ.

The doublet distribution on each wake is uniform and the wake source singularity τ is zero,

$$\mu_q = \text{const}, \quad \tau_q = 0, \quad q \in W_j \text{ for } j = 1, \ldots, n_c \tag{29}$$

The choice of these wake singularities [Eq. (29)] yields a continuous velocity field across W_j and a constant jump in potential across each wake line.

Limited Space Discretization

The integral representation of φ given by Eq. (10) allows us to reformulate the complete problem given by Eqs. (1-7) in terms of the unknown singularity distributions μ and σ, as was done above for the boundary conditions. To complete this reformulation, we substitute Eq. (10) in the governing equation (1). The result expresses the source singularity distribution σ,

$$\sigma(x, y) = a^2 \Phi_{xx} + \Phi_{yy} \tag{30}$$

in terms of the exact solution Φ. This relation shows that the local source strength σ is zero if Eq. (1) reduces locally to the Laplace or Prandtl-Glauert (P-G) equation. If σ is small over a part of the domain D such that its effect on the potential [Eq. (10)] is negligible, we may omit that part of the computational domain. Limited space discretization need not lower the accuracy of the solution, provided the error due to omitted sources is of the same order as the discretization errors of the numerical algorithm. This implies that the required size of the space to be discretized does increase with decreasing mesh or panel size. However, it should be mentioned that the flow velocities at the edges of the space mesh are continuous, in spite of a discontinuity in the strength of the source singularity distribution at these edges.

The actual magnitude of the source strength σ in subsonic flow regions is obtained by rewriting Eq. (1) in streamline coordinates and subtracting Eq. (30) from it. Thus, we obtain

$$\sigma = M^2 \Phi_{ss} - M_\infty^2 \Phi_{xx} \tag{31a}$$

for the Prandtl-Glauert operator and

$$\sigma = M^2 \Phi_{ss} \tag{31b}$$

for the Laplace operator, with M denoting the local Mach number and Φ_{ss} the local rate of change, in streamline direction s, of the velocity.

In case of the P-G operator [Eq. (31a)], σ is small if the magnitude of the perturbation velocity $|\vec{\nabla}\varphi|$ is small compared to the freestream velocity u_∞, even if the Mach number M_∞ is high subsonic.

On the other hand, if we opt for the Laplace operator in Eq. (8), the local source singularity σ [Eq. (31b)] will be small if the local Mach number is small compared to unity, as is the case over the largest part of the domain D for flows at low freestream Mach number M_∞. This second choice is important for airplane takeoff and landing configurations because the

perturbation velocity does not need to be small, as is the case for the Prandtl-Glauert option. For such high-lift flows, the nonlinear domain can be limited to a small part of the flow domain without degrading the accuracy of the full potential solution.

Full Potential Equation Formulation

One could treat Eq. (1) as a modified Poisson equation,

$$a\vec{\nabla}\cdot\vec{\nabla}\Phi=\sigma \tag{32}$$

with σ being specified by Eq. (31a) or (31b). Discretization of Eq. (31a) or (31b) for transonic flows with shock waves does not appear attractive, however, because Eq. (32) is not a conservation form.

A more direct approach is to disregard Eqs. (31) and to treat the full potential equation (1) directly by the well-established fully conservative finite-volume technique[11] before substitution of the integral representation [Eq. (10)]. This technique transforms Eq. (1) to a new set of coordinates ξ,η in the computational space and yields

$$\vec{\nabla}_{\xi,\eta}\cdot(\rho hG^{-1}\vec{\nabla}_{\xi,\eta}\Phi)=0 \tag{33}$$

where the del operator in the computational space with unit vectors $\hat{e}_\xi,\hat{e}_\eta$ is given by

$$\vec{\nabla}_{\xi,\eta}=\hat{e}_\xi\frac{\partial}{\partial\xi}+\hat{e}_\eta\frac{\partial}{\partial\eta} \tag{34}$$

the Jacobian matrix of the transformation by

$$H=\begin{bmatrix} x_\xi & x_\eta \\ y_\xi & y_\eta \end{bmatrix} \tag{35}$$

and its determinant by $h=\det(H)$. The metric tensor of the ξ,η coordinate system is given by the matrix

$$G=H^TH \tag{36}$$

In the present transonic panel method, we employ the fully conservative finite-volume technique to discretize Eq. (33), allowing the shock waves to be captured without compromising the ability to limit the size of the computational domain in which Eq. (33) needs to be discretized and solved.

IV. Numerical Algorithm

Finite Volume Scheme

Let the computational space be discretized in a number of uniform finite volumes with volume faces of length 1, and let the subscript pairs $(i+\frac{1}{2}, j)$, $(i-\frac{1}{2}, j)$, $(i, j+\frac{1}{2})$, and $(i, j-\frac{1}{2})$ refer to evaluation at the midpoints of the four volume faces of the finite volume (i,j) with its center at (ξ_j,η_j). Then, we may write a standard difference approximation to Eq. (33) in terms of the components of the split flux $\tilde{m}$

$$\tilde{m}^1_{i+\frac{1}{2},j}-\tilde{m}^1_{i-\frac{1}{2},j}+\tilde{m}^2_{i,j+\frac{1}{2}}-\tilde{m}^2_{i,j-\frac{1}{2}}=0 \tag{37}$$

These split-flux components, $\tilde{m}^k$ $(k=1,2)$, at the midpoints of the volume faces are obtained by splitting the components of the unmodified flux m^k $(k=1,2)$ of Eq. (33),

$$m^1\hat{e}_\xi+m^2\hat{e}_\eta=\rho hG^{-1}\vec{\nabla}_{\xi,\eta}\Phi \tag{38}$$

where the contravariant velocity components Φ_ξ,Φ_η at the midpoints of the volume faces are approximated by second-order accurate central differences in terms of potentials at volume centers $\Phi_{i,j}$. The density ρ and h,G^{-1} in Eq. (38) are also evaluated at the volume-face midpoints. Before introducing the splitting procedure of m^1 and m^2, let us define the mass flux

$$Q=\rho[\vec{\nabla}_{\xi,\eta}\Phi\cdot(G^{-1}\vec{\nabla}_{\xi,\eta}\Phi)]^{\frac{1}{2}} \tag{39}$$

at the midpoints of the volume faces and its maximum, sonic value by

$$Q^*=\frac{1}{M_\infty}\left[\left(\frac{2}{\gamma+1}\right)\left(1+\frac{\gamma-1}{2}M_\infty^2\right)\right]^{(\gamma-1)/(2\gamma+2)} \tag{40}$$

The flux components m^1 or m^2 are subsequently split into three monotonic parts according to

$$m^k=\frac{Q^*}{Q}m^k-(\Delta m^+)^k-(\Delta m^0)^k \tag{41a}$$

with

$$(\Delta m^+)^k=\frac{Q^*}{Q}m^k-\begin{cases} m^k & \text{if } M\geq 1 \\ \dfrac{Q^*}{Q}m^k & \text{if } M<1 \end{cases} \tag{41b}$$

and

$$(\Delta m^0)^k=\frac{Q^*}{Q}m^k-\begin{cases} m^k & \text{if } M<1 \\ \dfrac{Q^*}{Q}m^k & \text{if } M\geq 1 \end{cases} \tag{41c}$$

for $k=1$ or 2.

This splitting allows us to apply upwind differencing to $(\Delta m^+)^k$, which is nonzero only for supersonic points. The components of the split flux $\tilde{m}$ at volume face c are given by,

$$\tilde{m}^k_c=\frac{Q^*}{Q_c}m^k_c-(\Delta m^+)^k_{\text{up}}-(\Delta m^0)^k_c,\quad k=1,2 \tag{42}$$

where the variables with subscript c refer to the midpoint of the volume face under consideration, while the subscript "up" refers to a corresponding upstream volume-face midpoint, the wind direction being given by the sign of the flux component m^k. This splitting is identical with the Engquist and Osher[12] scheme, except for the scaling factor Q^*/Q introduced by Boerstoel,[14] needed for generalization to two or three dimensions.

The splitting given by Eq. (42) can be refined at shock points if we replace Eq. (42) by (for $k=1,2$)

$$\tilde{m}^k_c=\frac{Q^*}{Q_c}m^k_c-\begin{cases} (\Delta m^+)^k_{\text{up}} & \text{if } Q_c>Q_{\text{up}} \\ (\Delta m^0)^k_c & \text{if } Q_c\leq Q_{\text{up}} \end{cases} \tag{43}$$

if and only if $M_c<1$ and $M_{\text{up}}\geq 1$.

This modification of the Engquist and Osher scheme [Eq. (42)] at shock points results in the Godunov scheme as shown by Van Leer.[13] This Godunov-type scheme has been employed because it yields a minimum number of volume-face midpoints in the shock layer, at most one, and excludes the possibility of expansion shocks, while other widely used difference schemes do not exclude expansion shocks, as found by other authors.[13,14]

Panel Scheme

We approximate the source singularity distribution σ in the first integral of Eq. (10) by interpreting the finite volumes as

field panels over which the source strength is taken to be uniform. Panel-by-panel integration allows us to express the potential at the finite volume centers $\Phi_{i,j}$ in terms of the discrete values of the source singularity $\sigma_{i,j}$. Thus, in domain D we choose the finite volume centers as collocation points for the integral representation [Eq. (10)]. This choice yields a numerically stable scheme, as can be shown by linear stability arguments.

The remaining singularity distributions, τ and μ, are discretized by standard procedures,[15] including first-order correction terms yielding second-order accuracy of the boundary integrals in Eq. (10). Boundary panel midpoints are chosen as collocation points for the interior Dirichlet boundary conditions [Eq. (24)] and the derivatives of μ in the Kutta conditions [Eq. (28)] are approximated by one-sided differences of second-order accuracy.

These discrete approximations of Eq. (10) yield a matrix of aerodynamic influence coefficients (AIC), which expresses the linear relation between the potential at collocation points, i.e., finite volume centers and boundary panel midpoints, and the discrete singularity parameters of σ, τ, and μ.

Iterative Procedure

Let the system of linear and nonlinear equations be represented symbolically as

$$F(u) = 0 \tag{44}$$

where F is an n-dimensional column vector with algebraic functions as components and u an n-dimensional column vector with the unknown singularity parameters as components. Thus, Eq. (44) represents the nonlinear equations (37) and all linear ones [Eqs. (24) and (28)]. This system is solved by Newton's method

$$\left[\frac{\partial F}{\partial u}\right]^{(\nu)} (u^{(\nu+1)} - u^{(\nu)}) + F(u^{(\nu)}) = 0, \quad \nu = 1,2,\ldots \tag{45}$$

where the superscript ν indicates the Newton iteration index. Since the Jacobian matrix in Eq. (45) is computationally complex and fully populated, it is advantageous to write its factored form,

$$\left[\frac{\partial F}{\partial u}\right]^{(\nu)} = \left[\frac{\partial F}{\partial \phi}\right]^{(\nu)} \left[\frac{\partial \phi}{\partial u}\right] \equiv [B]^{(\nu)}\,[\mathrm{AIC}] \tag{46}$$

where ϕ represents a finite-dimensional column vector of potentials. The gradient matrix $B^{(\nu)}$, following from Eqs. (24), (28), and (37), is sparse and has a banded structure. The matrix of aerodynamic influence coefficients, following from the integral representation [Eq. (10)], is calculated only once because its elements are dependent only upon the geometric data of the configuration and the grid.

The system of linear equations (45) is solved iteratively. This iteration procedure embedded within each Newton step contains a relaxation scheme based on an approximate and incomplete lower-upper factorization technique of the full linear system [Eqs. (45)]. Similar relaxation schemes have been employed successfully by Oskam and Fray[16] as a smoothing operator in a fast multigrid method for solving the linear integral equations associated with higher-order accurate panel methods for incompressible potential flow. This experience suggests that it is feasible to accelerate the iterative solution algorithm for transonic panel methods by multigrid techniques; the present solutions of Eqs. (45) are obtained by relaxation at a single level of discretization, however.

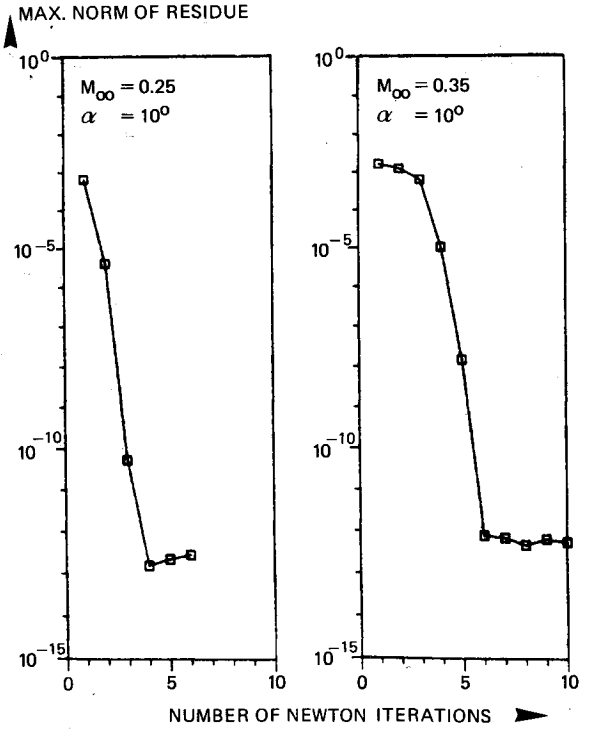

Fig. 2 Convergence of the maximum norm of the residue in Eqs. (44) for the paneling of Fig. 1.

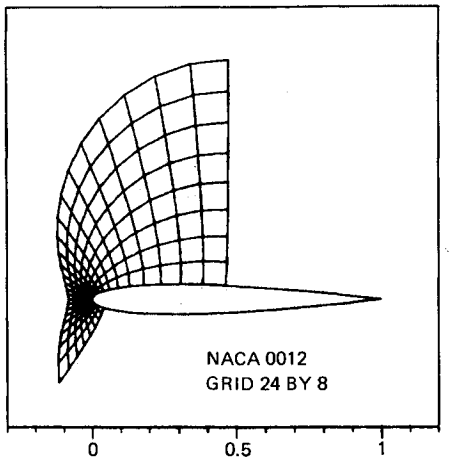

Fig. 1 Geometry of NACA 0012 airfoil (64 surface panels and 24 × 8 field panels).

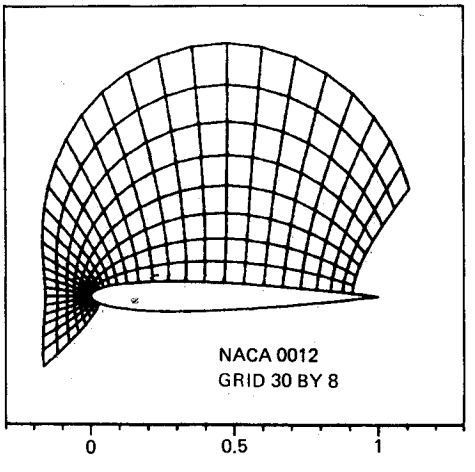

Fig. 3 Geometry of NACA 0012 airfoil (64 surface panels and 30 × 8 field panels).

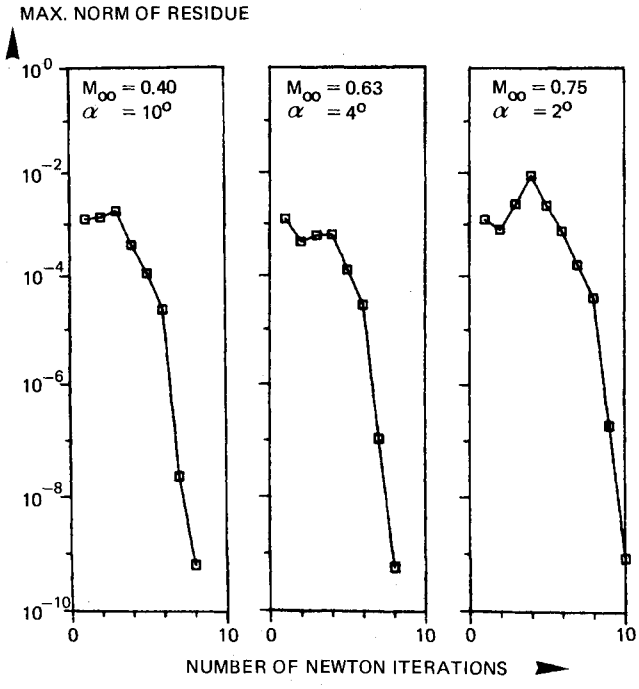

Fig. 4 Convergence of the maximum norm of the residue in Eqs. (44) for the paneling of Fig. 3.

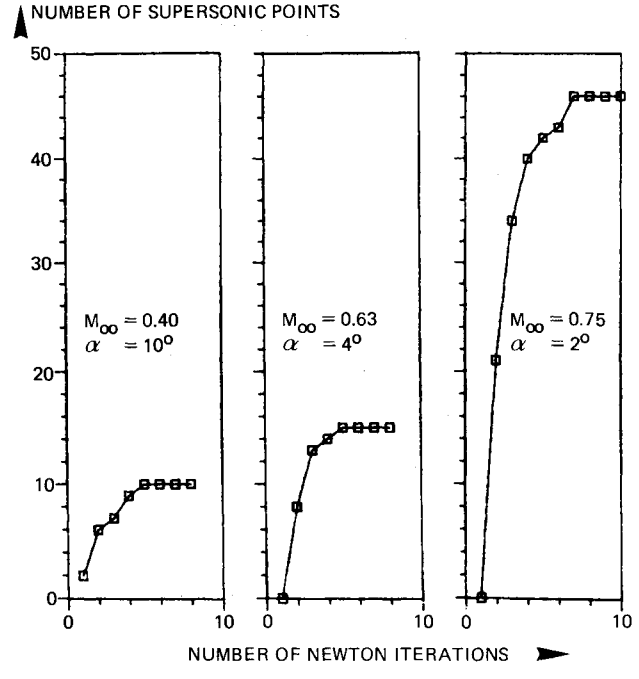

Fig. 5 Convergence of the number of supersonic points in the solution for the paneling of Fig. 3.

One of the questions associated with Newton's method [Eqs. (45)] concerns the requirement for an initial iterate "sufficiently close" to the true solution. This question will be discussed in Sec. V, where results illustrate the domain of attraction to u, taking the solution of the linear problem, with $\sigma = 0$, as initial iterate $u^{(1)}$.

V. Computational Results

In this section we briefly discuss some of the computational results obtained with the pilot code mentioned in the Introduction. The grid used in the first test problem is shown in Fig. 1. The NACA 0012 airfoil is discretized into 64 surface panels. The grid consists of 24×8 finite volumes or field panels.

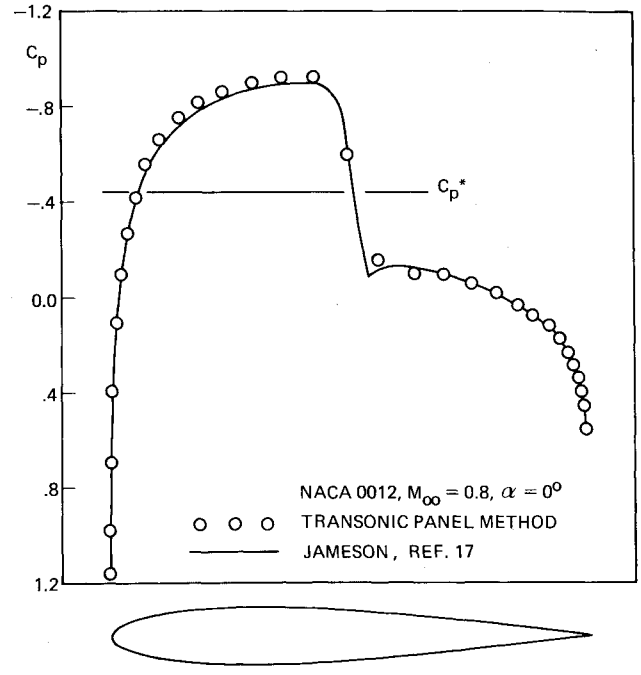

Fig. 6 Comparison of the pressure coefficients of the transonic panel method with potential flow results of Jameson.[17]

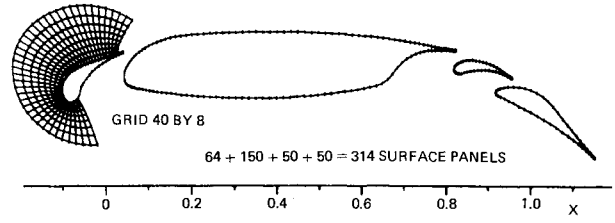

Fig. 7 Geometry of four-component airfoil ($n_c = 4$) with partial grid; total number of surface panels on the slat, wing, vane, and rear flap equals 314.

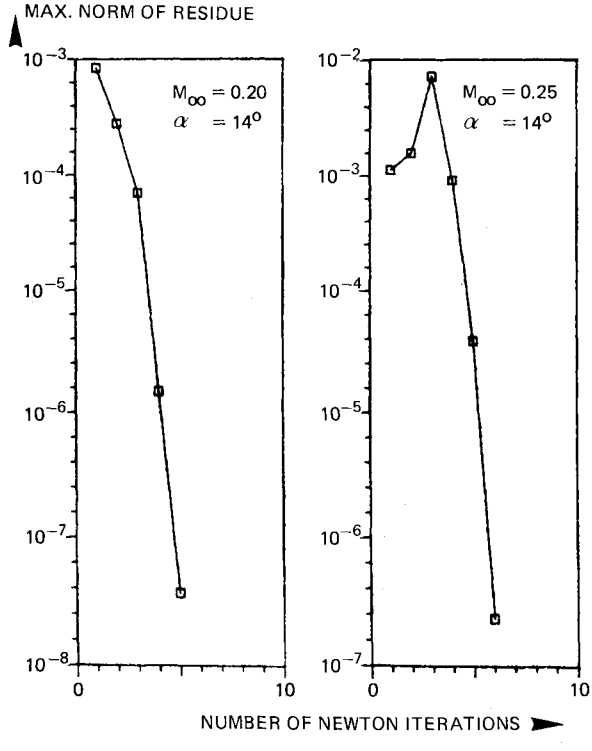

Fig. 8 Convergence of the maximum norm of the residue in Eqs. (44) for the paneling of Fig. 7.

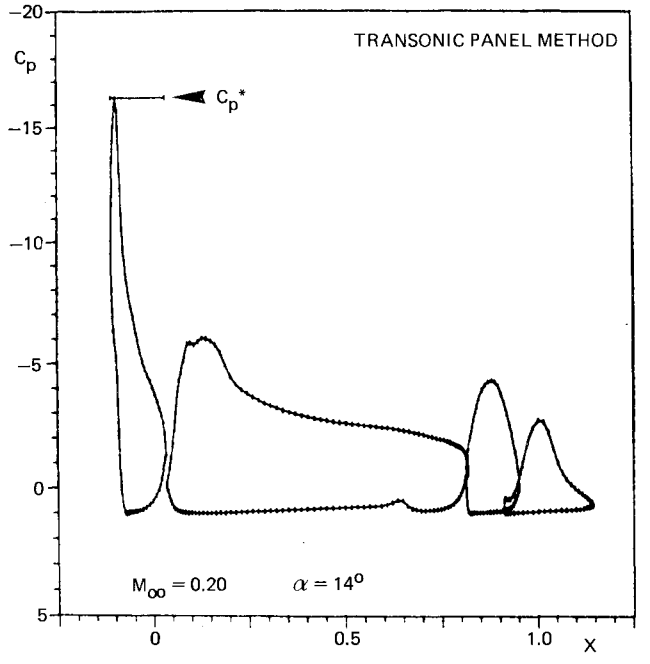

Fig. 9a Pressure coefficients C_p as a function of chordwise distance x for the paneling of Fig. 7; $M_\infty = 0.20$.

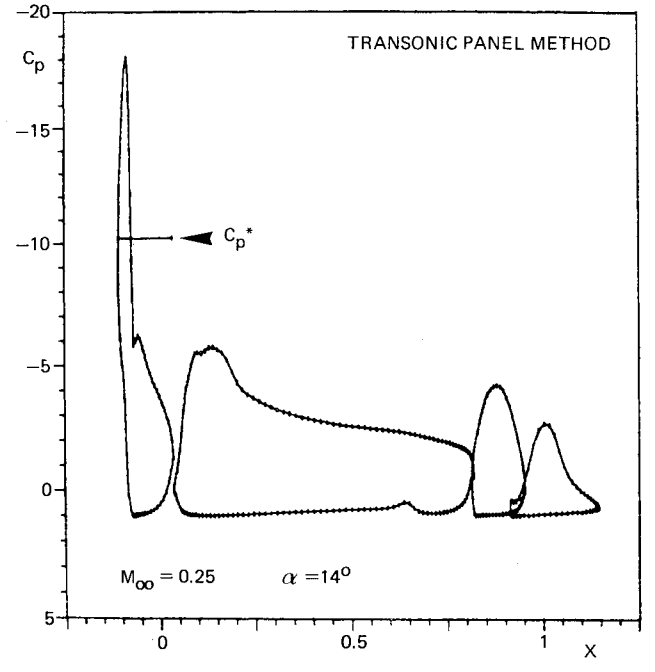

Fig. 9b Pressure coefficients C_p as a function of chordwise distance x for the paneling of Fig. 7; $M_\infty = 0.25$.

The convergence history of the maximum norm of the n-dimensional column vector of residues of Eq. (44) is shown in Fig. 2. The angle of attack α of the airfoil is equal to 10 deg, while the potential flow is computed for two freestream Mach numbers, $M_\infty = 0.25$ and 0.35, respectively. This increase in M_∞ from 0.25 to 0.35 is sufficient to generate supersonic flow locally around the airfoil nose. The convergence history for $M_\infty = 0.35$ is fast but not quadratic as for the completely subsonic case at $M_\infty = 0.25$. Convergence is halted when the machine round-off error level is reached.

The effect of the initial and subsequent iterates on the convergence of the Newton procedure is further illustrated by three computations using the paneling of Fig. 3, with 30×8 field panels. Three cases are considered. The convergence histories of the maximum norm are shown in Fig. 4 and the

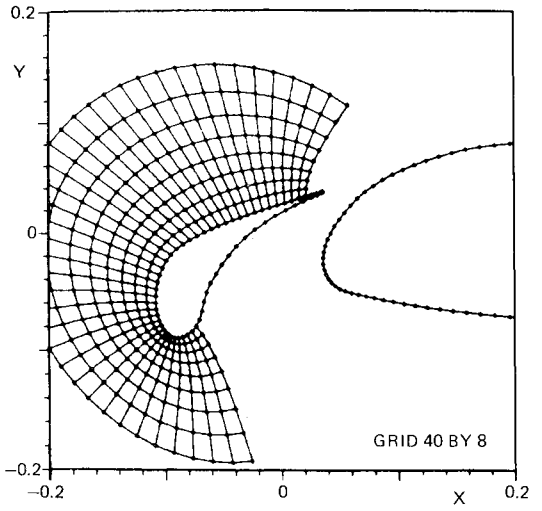

Fig. 10a Enlarged view of the partial grid around the slat of the four-component airfoil ($n_c = 4$).

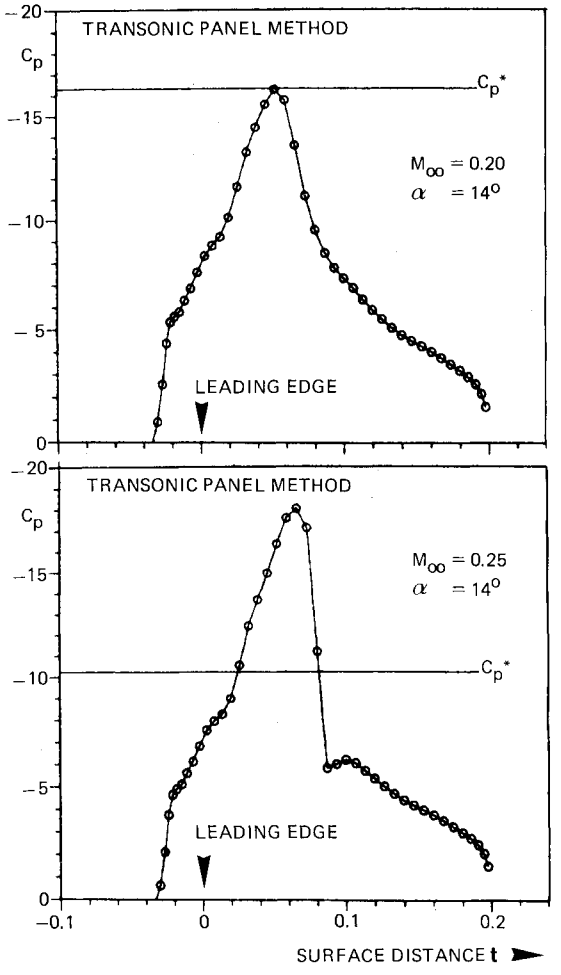

Fig. 10b Enlarged view of the pressure distribution on the slat as a function of the surface distance (upper side) for $M_\infty = 0.20$ and 0.25 (sonic value denoted by C_p^*).

corresponding developments of the number of supersonic points are displayed in Fig. 5. These results show that for the present transonic panel method the Newton iterations converge, even if the initial iterate is not close to the true solution. Comparing Figs. 4 and 5 shows that the convergence rate increases once the number of supersonic points has converged. The Newton procedure is stopped when the maximum norm of the residue vector is lower than 10^{-9}.

One of the standard test problems defined at a recent GAMM Workshop[17] is NACA 0012 at $M_\infty = 0.80$ and $\alpha = 0$ deg. This problem is solved with the present transonic panel method with a grid of 58×10 field panels. Comparison of the pressure distribution as a function of x/c with the fully conservative potential flow results of Jameson[17] is given in Fig. 6. This case ($M_\infty = 0.80$ and $\alpha = 0$ deg) shows no significant differences in the two sets of results, in comparison with the differences found between the results of other participants of the Workshop.[17]

As a last example, we will show results for the transonic flow around a four-component high-lift configuration (Fig. 7) with an angle of attack of 14 deg and at two freestream Mach numbers, $M_\infty = 0.20$ and 0.25. For these cases Newton's method converges within six iterations to a level of 10^{-6} for the maximum norm of the residue vector, see Fig. 8. The resulting pressure distributions are shown in Figs. 9a and 9b, where one may observe the development of a small pocket of supersonic flow as M_∞ increases from 0.20 to 0.25. Figure 10a shows an enlarged view of the slat and Fig. 10b the pressure distributions as a function of the correspondingly enlarged surface distance t. These pressures show a strong shock wave on the slat, which is critically important for analyzing the maximum lift capabilities of such configurations.

VI. Conclusions

The formulation of a new transonic panel method has been presented. The results of the pilot code version of this method show that transonic potential flows can be treated with the well-established fully conservative finite volume technique, while reducing the computational domain in which the full potential equation needs to be solved explicitly. The latter characteristic implies a significant reduction in the mesh generation effort required for transonic flow computations. Further developments of this new method are being directed toward lowering the computational effort required. These developments include multigrid techniques for the fast iterative solution of the system of nonlinear equations associated with panel methods, as well as fast procedures for the evaluation of integral representations.

Acknowledgments

The author would like to thank his colleagues at NLR, in particular Messrs. J. W. Slooff and W. J. Piers, for discussions on the present subject.

References

[1]Hess, J. L. and Smith, A. M. O., "Calculation of Nonlifting Potential Flow about Arbitrary Three-Dimensional Bodies," Douglas Aircraft Corp., Long Beach, Calif., Rept. ES40622, 1962.

[2]Luu, T. S. and Coulmy, G., "Method of Calculating the Compressible Flow Around an Aerofoil or a Cascade up to the Shockfree Transonic Range," *Computers and Fluids*, Vol. 5, 1977, pp. 261-275.

[3]Stricker, R., "Integral Equation Method for Calculation of the Fully Nonlinear Potential Flow about Arbitrary Section Shapes," Paper presented at the Euromech Colloquium 75, Rhode/Braunschweig, FRG, 1976.

[4]Piers, W. J. and Slooff, J. W., "Calculation of Transonic Flow by means of a Shock-Capturing Field Panel Method," AIAA Paper 79-1459, 1979.

[5]Hounjet, M. H. L., "Transonic Panel Method to Determine Loads on Oscillating Airfoils with Shocks," *AIAA Journal*, Vol. 19, May 1981, pp. 559-566.

[6]Wu, J. C., El-Refaee, M., and Lekoudis, S. G., "Solutions of the Unsteady Two-Dimensional Compressible Navier-Stokes Equations Using the Integral Representation Method," AIAA Paper 81-0046, 1981.

[7]Halsey, N. D., "Rapid, High-Order Accurate Calculation of Flows due to Free Source or Vortex Distributions," Paper 4, NASA Conference Publication 2201, Ames Research Center, Moffett Field, Oct. 1981.

[8]Johnson, F. T., James, R. M., Bussoletti, J. E., Woo, A. C., and Young, D. P., "A Transonic Rectangular Grid Embedded Panel Method," AIAA Paper 82-0953, June 1982.

[9]Slooff, J. W., "Some New Developments in Exact Integral Equation Formulations for Sub- and Transonic Potential Flow," National Aerospace Laboratory, Amsterdam, Rept. NLR MP 82024 U, 1982.

[10]Slooff, J. W., "Requirements and Developments Shaping a Next Generation of Integral Methods," National Aerospace Laboratory, Amsterdam, Rept. NLR MP 81007 U, 1981.

[11]Jameson, A. and Caughey, D. A., "A Finite-Volume Method for Transonic Potential Flow Calculations," *Proceedings of AIAA 3rd Computational Fluid Dynamics Conference*, AIAA, New York, 1977, pp. 35-54.

[12]Engquist, B. and Osher, S., "Stable and Entropy Satisfying Approximations for Transonic Flow Calculations," *Mathematics of Computation*, Vol. 34, No. 149, Jan. 1980, pp. 45-75.

[13]Van Leer, B., "On the Relation between the Upwind-Differencing Schemes of Godunov, Engquist & Osher and Roe," ICASE Rept. 81-11, March 1981.

[14]Boerstoel, J. W., "A Multigrid Algorithm for Steady Transonic Potential Flows Around Airfoils using Newton Iteration," *Journal of Computational Physics*, Vol. 48, No. 3, 1982, pp. 314-343.

[15]Hess, J. L., "Consistent Velocity and Potential Expansions for Higher-Order Surface Singularity Methods," McDonnell Douglas Corp., Long Beach, Calif., Rept. MDCJ6911, June 1975.

[16]Oskam, B. and Fray, J. M. J., "General Relaxation Schemes in Multigrid Algorithms for Higher-Order Singularity Methods," *Journal of Computational Physics*, Vol. 48, No. 3, 1982, pp. 423-440.

[17]Rizzi, A. and Viviand, H., eds., "Numerical Methods for the Computation of Inviscid Transonic Flows with Shock Waves," *Notes on Numerical Fluid Mechanics*, Vol. 3, Friedr. Vieweg & Sohn, Braunschweig, FRG, 1981.